Neutron powder diffraction of rhombohedral Y2Fe17 and Y2Fe17N3.1

doi: 10.1103/PhysRevB.55.11414

Neutron powder diffraction of rhombohedral Y_2Fe_{17} and $Y_2Fe_{17}N_{3.1}$

K. Koyama
Faculty of Integrated Arts and Sciences, Hiroshima University, Higashi-hiroshima 724, Japan

T. Kajitani
Department of Applied Physics, Tohoku University, Sendai 980-77, Japan

Y. Morii
Advanced Science Research Center, Japan Atomic Energy Research Institute, Tokai, Ibaraki 319-11, Japan

H. Fujii and M. Akayama
Faculty of Integrated Arts and Sciences, Hiroshima University, Higashi-hiroshima 724, Japan

(Received 8 November 1996)

High resolution neutron powder diffraction experiments were carried out on rhombohedral Y_2Fe_{17} and the nitride $Y_2Fe_{17}N_{3.1}$ at 10 K. The diffraction data were analyzed by the recently refined Rietveld method. The results obtained indicate that nitrogen atoms fully occupy the $9e$ site (99.5%) and that a small amount of N atoms locate at the $18g$ site (3.9%). The introduction of N atoms into Y_2Fe_{17} leads to strong modification of the Fe magnetic moments. The magnetic moment of the $18f$-Fe atoms which are the nearest to the $9e$-N atoms in nitride is the lowest value ($\sim 2.0\mu_B$), whereas the $6c$-Fe atoms being the farthest from the $9e$-N atoms have the highest moment ($\sim 2.9\mu_B$). The difference of Fe moments on nonequivalent sites is discussed on the basis of the Fe-Fe and Fe-N bond distances. The obtained results are compared with the results of electronic band-structure calculation. [S0163-1829(97)12017-3]

I. INTRODUCTION

In general, the R_2Fe_{17} (R=rare earth) intermetallic compounds crystalline in the rhombohedral Th_2Zn_{17}-type structure for light rare earths or the hexagonal Th_2Ni_{17}-type structure for heavy rare earths and yttrium.[1] Among them, the compounds with R=Ce, Gd, Tb, and Y crystallize in either the rhombohedral or hexagonal structure depending on the annealing temperature.[1]

The R and Fe magnetic moments in the R_2Fe_{17} compounds couple ferromagnetically with each other for R =light rare earth and ferrimagnetically for R=heavy rare earth, because the exchange interaction between the R and Fe spins is antiferromagnetic. As a result of ferromagnetic coupling between the R moment for light rare earths and Fe moment of $\sim 2\ \mu_B$ per Fe atom, the light rare-earth compounds are expected to have larger saturation magnetic moments than the total Fe sublattice moment, 34 μ_B/f.u. On the other hand, the Curie temperature T_C is around room temperature. The reason for the low T_C in the R_2Fe_{17} compounds is believed to be due to a too large overlap of the wave functions of Fe $3d$ electrons; that is to say, the Fe-Fe distance is too short for stable ferromagnetism in these compounds.[2] In addition, the R_2Fe_{17} compounds do not have uniaxial anisotropy at room temperature. Therefore, the R_2Fe_{17} compounds had not been recognized as a candidate for hard magnetic materials.

In 1990, Coey and Sun reported that the introduction of nitrogen atoms into the R_2Fe_{17} compounds led to remarkable increases in the T_C and magnetic moments of the Fe sublattice accompanied by a large increase in unit cell volume ($\sim 7\%$) without changing the their crystal structures.[3] Especially, the fully nitrided $Sm_2Fe_{17}N_{2.94}$ has been reported to have a high Curie temperature (T_C=746 K), a large saturation magnetization (M_s=1.54 T), and a strong uniaxial anisotropy ($\mu_0 H_A$=21.0 T) at room temperature.[4] Since then, the nitride $Sm_2Fe_{17}N_3$ has been regarded as a suitable candidate for high-performance permanent magnets. Many experimental studies have been performed to clarify the basic magnetic properties of the interstitially modified compounds $R_2Fe_{17}N_3$, which are summarized in a review article.[5] ^{57}Fe Mössbauer[6,7] and neutron powder diffraction[2,8–18] experiments have also been carried out to study the microscopic influence of interstitial nitrogen atoms on the Fe magnetic moments, and the results have often been compared with those of band-structure calculations.[2,19,20] From these many studies, it has been suggested that the drastic improvement in intrinsic magnetic properties for R_2Fe_{17} upon nitrogenation closely relates both to the interstitial sites occupied by N atoms and to the concomitant lattice expansion.

Neutron diffraction is the most useful method to microscopically study the crystallographic and magnetic structures. Until now, the neutron diffraction studies for $Ce_2Fe_{17}N_x$,[8] $Nd_2Fe_{17}N_x$,[2,8–15] $Pr_2Fe_{17}N_x$,[16] $Th_2Fe_{17}N_x$,[17] the hexagonal $Y_2Fe_{17}N_x$,[2,9,11,12] and two phases $Y_2Fe_{17}N_x$ ($0 \leqslant x \leqslant 4.5$) (Ref. 18) have been carried out. From the above experiments, it has been claimed that the N atoms mainly occupy the $9e$ site for the rhombohedral structure or the $6h$ site for the hexagonal one. In particular, the neuron diffraction study on Y_2Fe_{17} and $Y_2Fe_{17}N_x$ with a nonmagnetic Y is suitable to elucidate the magnetism of the Fe sublattice in the interstitially modified R_2Fe_{17}. However, in detail, the influence of interstitial N atoms on the Fe magnetic moments

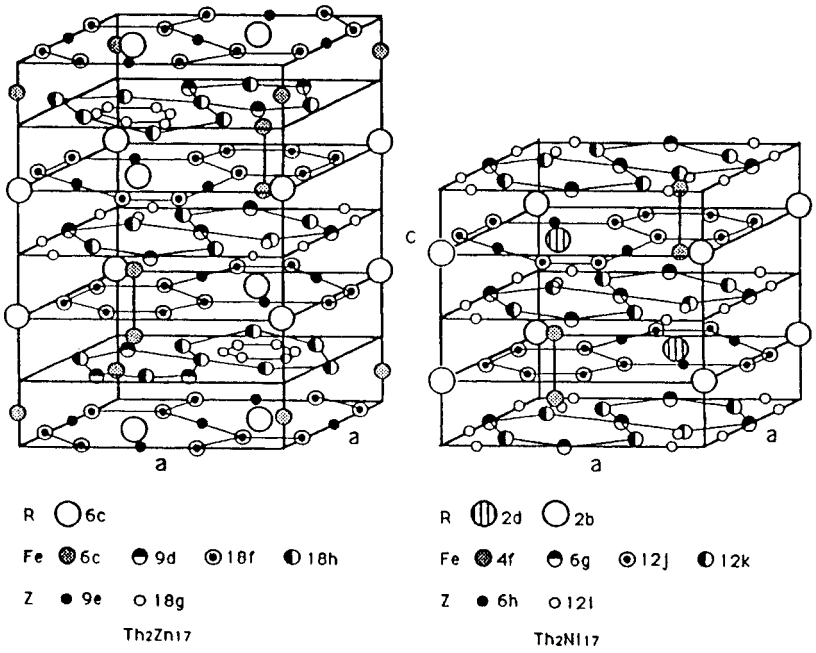

FIG. 1. Crystal structures of R_2Fe_{17}: rhombohedral Th_2Zn_{17} type (left) and hexagonal Th_2Ni_{17} type (right), showing the rare-earth sites (R), iron sites (Fe), and the interstitial sites (Z).

in the rhombohedral $Y_2Fe_{17}N_x$ has not been reported yet because of the difficulty to obtain a single-phased sample. Furthermore, the neutron diffraction studies on $Y_2Fe_{17}N_x$ with the same crystal structure as in $Sm_2Fe_{17}N_3$ are easier for analysis relative to those with the hexagonal one, because the rhombohedral compounds have virtually no partial disorder. So far, some partial disorders along the c axis have been reported in the hexagonal ones such as Lu_2Fe_{17},[21] Ho_2Fe_{17},[22] and Y_2Fe_{17}.[2,9,12]

In our previous work,[23] we have synthesized a single-phase sample with the rhombohedral structure of Y_2Fe_{17} by long annealing at higher temperature. Furthermore, we have revealed that the high-quality $R_2Fe_{17}N_3$ nitrides with little segregation of α-Fe phase could be synthesized by means of a high-pressure nitrogenation technique.[23,24] In this paper, we report the results of high-resolution neutron powder diffraction studies at 10 K on the rhombohedral Y_2Fe_{17} and the $Y_2Fe_{17}N_{3.1}$ nitride synthesized by the high-pressure nitrogenation for obtaining information on the change of microscopic magnetism of the Fe sublattice upon nitrogenation.

II. CRYSTAL STRUCTURES

The rhombohedral Th_2Zn_{17}-type structure (space group $R\bar{3}m$) and hexagonal Th_2Ni_{17}-type structure ($P6_3/mmc$) are illustrated in Fig. 1. Both of the structures are derived from a hexagonal $CaCu_5$-type structure by the ordered substitution with a pair of Fe atoms (dumbbell) for each third rare-earth atom in the basal plane:

$$3(RFe_5) - R + 2Fe(\text{dumbbell}) \rightarrow R_2Fe_{17}. \quad (1)$$

When these substituted layers are stacked in the sequence $ABCABC\ldots$ along the c axis on the $CaCu_5$-type structure, the rhombohedral Th_2Zn_{17}-type structure is realized. If the staking sequence is, instead, $ABAB\ldots$ along the same direction, then the hexagonal Th_2Ni_{17}-type structure is formed. However, in actual structure of the hexagonal R_2Fe_{17} compounds with R=Lu, Ho, and Y, partial disorder has been observed.[2,9,12,21,22] The partial disorder of the hexagonal structure is induced by the exchange of some of the R atoms at the $2b$ site for Fe-dumbbell atoms and Fe-dumbbell atoms at the $4f$ site for the R atoms.

The rhombohedral compound has only one crystallographically nonequivalent rare-earth site ($6c$ site), while the hexagonal compound has two crystallographically nonequivalent rare-earth sites ($2b$ and $2d$ sites). These sites are, however, characterized by a quite similar local atomic arrangement of Fe atoms and by a slight different arrangement of the rare-earth atoms. As is seen in Fig. 1, the hexagonal $4f$, $6g$, $12j$, and $12k$ sites correspond to the rhombohedral $6c$, $9d$, $18f$, and $18h$ sites with respect to crystallographic configuration, respectively. The neutron diffraction studies have revealed that the N atoms mainly occupy the $9e$ site in the rhombohedral structure or the $6h$ site in the hexagonal structure (see Fig. 1).[2,8–16] Among them, some authors have suggested, as a second interstitial site for nitrogen occupation, the $18g$ site for the rhombohedral structure or the $12i$ site for the hexagonal structure.[2,9,12,13,15]

III. EXPERIMENTAL PROCEDURE

A. Sample preparation and magnetic measurements

The host compound Y_2Fe_{17} was prepared by arc-melting the starting elements of 99.99% purity under a flowing Ar gas. The ingot was remelted several times to ensure its homogeneity. Subsequently, the as-melted ingot was wrapped by tantalum foil and sealed in evacuated quartz tubes. After annealing it at 1393 K for 2 weeks, the ingot was quenched in water. The annealed ingot was pulverized into fine powder less than 20 μm in diameter in a glove box with an Ar gas atmosphere. Nitrogenation was performed by heating the powder at 713 K for 24 h under a high-purity (99.9999%)

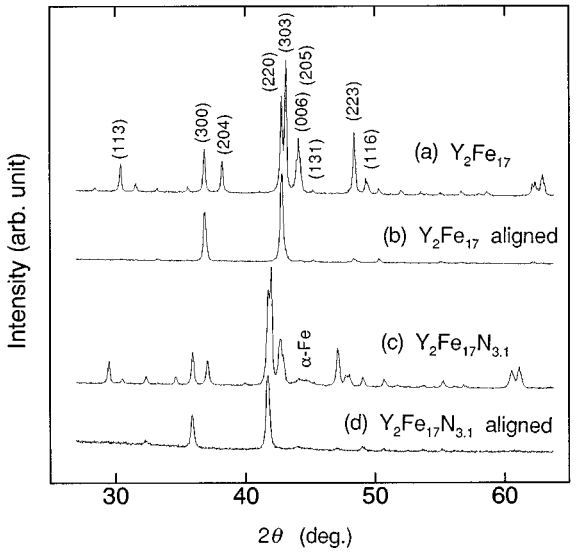

FIG. 2. X-ray diffraction patterns of Y_2Fe_{17} and $Y_2Fe_{17}N_{3.1}$ at room temperature using Cu $K\alpha$ radiation. (a) and (c) are for the nonaligned powder. (b) and (d) are for the aligned powder along the direction parallel to x-ray scattering vector at room temperature.

N_2 gas pressure of 6 MPa. The nitrogen concentration was estimated from the increase in mass of the sample after the nitrogenation, as an average value of 3.1 ± 0.1 N atoms per formula unit Y_2Fe_{17}.

In order to check the easy axis of magnetization and impurity phases in the host and nitride samples, powder x-ray diffraction (XRD) studies were carried out using an aligned powder in a magnetic field of 1.6 T at room temperature using Cu $K\alpha$ radiation. Magnetization was measured with a vibrating sample magnetometer in applied fields up to 1.6 T in a temperature range from 4.2 to 300 K using a electromagnet.

B. Neutron powder diffraction experiments and data analysis

Neutron powder diffraction experiments were carried out at 10 K using the High Resolution Neutron Diffractometer (HRPD) at JRR-3M of Japan Atomic Energy Research Institute. In the HRPD detector bank, 64 ^{3}He counters were placed at every 2.5° of diffraction angle.[25] The collimation of 6′-20′-6′ from the first through the third collimator was kept through the experiment. The samples were contained in a vanadium can with 10 mm diameter and 30 mm height. All data were taken with thermal neutron radiation at $\lambda=1.823$ Å (from a Ge 331 monochromator) in the 2θ range from 5° to 165° step size 0.05°. Intensity data from $2\theta=10°$ to 153° were used in the structure refinements using RIETAN-94,[26,27] which was developed for angle-dispersive x-ray and neutron powder data. RIETAN can analyze the data taken from mixtures of two or more phases, and can analyze magnetic structures with collinear spin arrangements. The neutron scattering lengths used for the refinement were $b_Y=7.750$, $b_{Fe}=9.540$, and $b_N=9.360$ in unit of 10^{-15} m. We adopted an analytical approximation to magnetic form factor for Fe and Y, which was taken from Ref. 28. Goodness of the fit between the observed and calculated patterns was indicated by the reliability factors R_p, R_I, and R_F, with

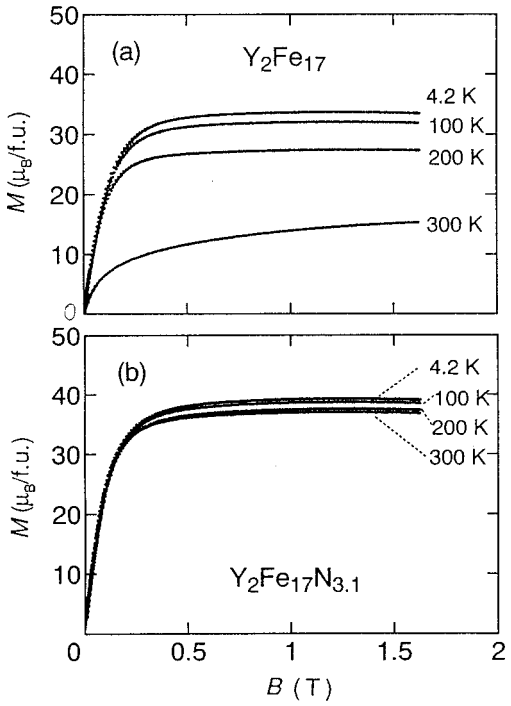

FIG. 3. Magnetization curves along the direction parallel to the magnetically aligned axis for Y_2Fe_{17} (a) and $Y_2Fe_{17}N_{3.1}$ (b).

$$R_p=\frac{\Sigma|y_i(o)-y_i(c)|}{\Sigma y_i(o)},$$

$$R_I=\frac{\Sigma|I_k(o)-I_k(c)|}{\Sigma I_k(o)},$$

and

$$R_F=\frac{\Sigma|\sqrt{I_k(o)}-\sqrt{I_k(c)}|}{\Sigma\sqrt{I_k(o)}},$$

where $y_i(o)$ and $y_i(c)$ are the observed and the calculated intensities, respectively, and $I_k(o)$ and $I_k(c)$ are integrated intensities of the observed kth peak and the calculated one, respectively.

IV. RESULTS

Figure 2 shows the nonaligned and aligned XRD patterns of Y_2Fe_{17} and $Y_2Fe_{17}N_{3.1}$ at room temperature using Cu $K\alpha$ radiation. As is evident from these x-ray profiles, the XRD pattern of the Y_2Fe_{17} host compound is almost a single phase of the rhombohedral structure with no trace of α-Fe phase ($2\theta=44.7°$). The nitride $Y_2Fe_{17}N_{3.1}$ is also confirmed to be almost single phase except for a very small amount of α-Fe phase. The XRD pattern of the nitride shifts to lower angle, indicating that the lattice expands without changing the rhombohedral structure upon nitrogenation. In order to determine the easy axis of magnetization (EAM), the XRD patterns were examined for the magnetically aligned powder

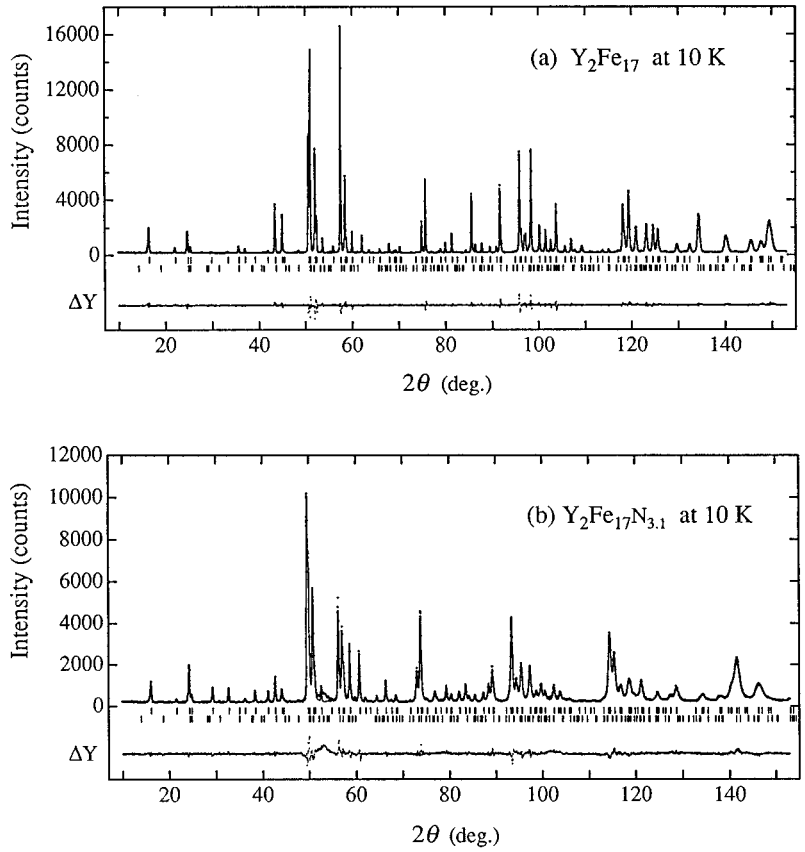

FIG. 4. Neutron powder diffraction patterns of Y_2Fe_{17} (a) and $Y_2Fe_{17}N_{3.1}$ (b) at 10 K. The dots and line correspond to the observed and calculated patterns, respectively. The lower part is the difference pattern (observed and calculated). The calculated peak positions of the rhombohedral and the hexagonal phases are indicated by the first and second bars, respectively.

along the direction parallel to the scattering vector at room temperature, which are shown in Figs. 2(b) and 2(d). Judging from the clear enhancement of the (300) and (220) peaks of Y_2Fe_{17} and $Y_2Fe_{17}N_{3.1}$, we concluded that the EAM of both the host and nitride was in the ab plane at room temperature. Furthermore, in order to examine the EAM below room temperature, we measured the magnetization curves along magnetically aligned axis for Y_2Fe_{17} and $Y_2Fe_{17}N_{3.1}$ in the temperature range from 4.2 to 300 K, which are shown in Fig. 3. Considering from the aligned XRD patterns in Fig. 2 and the smooth magnetization curves for all the temperature ranges in Fig. 3, the EAM of both the host and nitride was regarded as being in the same ab plane in the temperature range from 4.2 to 300 K as at room temperature.

Figure 4 shows the neutron diffraction patterns of Y_2Fe_{17} and $Y_2Fe_{17}N_{3.1}$ at 10 K. The dots and lines in the figures correspond to the observed intensities and calculated patterns, respectively. Since a very weak peak ($2\theta=48.8°$) corresponding to (203) of the hexagonal structure is confirmed, the refinements of the diffraction patterns of the host and nitride were performed assuming that the sample contains a very small amount of the hexagonal phase in addition to a large amount of the rhombohedral phase.

For the rhombohedral structure, the lattice parameters used as initial values were those obtained by XRD studies at room temperature, and the coordinates of atoms were taken from the results for Nd_2Fe_{17} reported by Kajitani *et al.*[13] For the hexagonal structure, the starting structural model without partial disorder was set on the basis of the hexagonal Y_2Fe_{17} reported by Yelon and Hadjipanayis.[12] With respect to the refinement of the magnetic moments, we assumed that the Y and N moments are $0\mu_B$, and that the Fe moments are collinear within the ab plane. The initial values of the Fe magnetic moments were taken as average moment obtained by magnetization measurement. The Fe moment at each site in the hexagonal structure was constrained to be the same value as that at each equivalent site in the rhombohedral structure. Parameters were refined in the following order: (1) background, scale, and profile parameters: (2) structural parameters of the rhombohedral phase: (3) structural parameters of the hexagonal phase: and finally, we refined (4) all parameters including magnetic moments and isotropic-thermal parameters.

The obtained structural data are summarized in Table I. As is seen in Fig. 4(a), the calculated patterns are in very good agreement with the observed patterns. From the results of the refinements, we found that the hexagonal phase is contained about 4% in the sample.

For the nitride $Y_2Fe_{17}N_{3.1}$, a small and broad peak corresponding to α-Fe segregation upon nitrogenation appears around $2\theta=53.4°$. In the first step, the analysis of the nitride $Y_2Fe_{17}N_{3.1}$ was performed assuming three phases (rhombohedral, hexagonal, and α-Fe phases) and using the whole data. The mass fraction of α-Fe was estimated to be about 5% in the sample, but we had the difficulty of getting a good profile fitting because of a too broad peak of α-Fe phase. Therefore, the refinements of the nitride were performed except for data in the 2θ range from 52.5° to 54.5°. Furthermore, the refinements were carried out by assuming the following two different models: (1) The N atoms occupy only

TABLE I. Refined parameters of rhombohedral and hexagonal phase for Y_2Fe_{17} at 10 K. n is the occupation factor; x, y, and z are the fractional coordinate; B is the isotropic thermal parameter (Å^2); and m is the magnetic moment (μ_B/atom). Numbers in parentheses are the *statistical* error given by the refinement program.

Y_2Fe_{17}		10 K		$R_p=5.62\%$			
Rhombohedral			$R_I=3.16\%$	$R_F=1.83\%$			
$a=8.5003(1)$ Å			$c=12.4294(1)$ Å				
Atom	Site	n	x	y	z	B	m
Y	6c	1.0	0	0	0.3413(6)	0.61(2)	
Fe(1)	6c	1.0	0	0	0.0960(4)	0.310(1)	2.23(5)
Fe(2)	9d	1.0	0.5	0	0.5	0.310	1.88(6)
Fe(3)	18f	1.0	0.2954(3)	0	0	0.310	1.94(2)
Fe(4)	18h	1.0	0.1672(2)	−0.1672	0.4910(2)	0.310	1.87(4)
Hexagonal				$R_I=5.43\%$	$R_F=3.54\%$		
$a=8.4659(6)$ Å			$c=8.3232(7)$ Å				
Atom	Site	n	x	y	z	B	m
Y	2b	1.0	0	0	0.25	0.61	
Y	2d	1.0	0.3333	0.6667	0.75	0.61	
Fe(1)	4f	1.0	0.3333	0.6667	0.108(7)	0.310	2.23
Fe(2)	6g	1.0	0.5	0	0	0.310	1.88
Fe(3)	12j	1.0	0.332(6)	0.961(5)	0.25	0.310	1.94
Fe(4)	12k	1.0	0.166(3)	0.332	0.988(4)	0.310	1.87

the 9e interstitial sites in the rhombohedral structure (one-site model) and (2) the N atoms occupy both the 9e and 18g interstitial sites (two-site model). In both models, the refined occupation of the N atoms in the 6h and 12i interstitial sites in the hexagonal structure was constrained to be the same as that on the corresponding 9e and 18g sites in the rhombohedral structure, respectively. Adopting the one-site model for the nitride at 10 K, the R factors reached $R_p=6.53\%$, $R_I=3.42\%$, and $R_F=2.31\%$, and the refined occupation of the N atoms became 1.004(7). On the other hand, the R factors for the two-site model at 10 K were $R_p=6.12\%$, $R_I=2.96\%$, and $R_F=1.97\%$, and the refined occupation of the N atoms on the 9e and 18g interstitial sites was 0.995(5) and 0.039(2), respectively. Here we adopted the two-site model, because the R factors for the two-site model were reasonably smaller than those for the one-site model. The refined structure data are summarized in Table II. The lattice parameters a and c at 10 K increase by 2.0% and 2.4%, respectively, by nitrogenation. The chemical formula of the nitride determined from the occupation factors becomes $Y_2Fe_{17}N_{3.2(1)}$. This nitrogen content deduced is also comparable with the value 3.1 ± 0.1 estimated from the increase in sample mass. From the structure refinements for $Y_2Fe_{17}N_{3.1}$, we can conclude that N atoms fully occupy the 9e site and a part of N atoms also occupy the 18g site in the nitride synthesized by high-pressure nitrogenation.

V. DISCUSSION

The Fe magnetic moments on crystallographically different sites in Y_2Fe_{17} and $Y_2Fe_{17}N_{3.1}$ at 10 K are summarized in Table III, together with the data obtained by magnetization measurements at 4.2 K (Fig. 3). The total magnetic moments m_T determined by the neutron diffraction experiment are in good agreement with the values obtained by magnetization measurements. As is evident from Table III, the site-dependent Fe moments for the host and nitride are observed. For Y_2Fe_{17} at 10 K, the Fe atoms at the 6c site have the largest moment, whereas the Fe atoms at the 9d and 18h sites have the smallest moments. On the other hand, the Fe moment at the 18f site in $Y_2Fe_{17}N_{3.1}$ is the lowest, but the magnetic moments of Fe at all the nonequivalent sites increase by the nitrogenation. As described in Sec. IV, we assumed in this analysis that Y and N had no magnetic moments. However, band-structure calculations[2,19,20,29–32] indicate that Y and N have small magnetic moments coupled antiparallel to Fe moments. Therefore, we also analyzed the diffraction data, assuming that Y had a small moment less than $0.5\mu_B$, it coupled antiparallel to the Fe moments, and N had no moment because of no information on magnetic form factor for N. However, the refinements gave almost no change on the Fe moment at each site compared with the above analysis even if Y had a small finite moment. In addition, the deduced total moment for the host and nitride did not well agree with those by the magnetization measurements, and no better R factors were obtained. Hence we concluded that the Y and N moments are negligibly small.

Both the interatomic and average Fe-Fe distances for the rhombohedral host and nitride at 10 K are listed in Tables IV and Tables V, respectively. On the basis of the Fe-Fe and Fe-N bond distances, the difference of the Fe magnetic moments in nonequivalent Fe sites in the host and nitride is understood as follows. For Y_2Fe_{17}, the highest Fe moment of $2.23\mu_B$ at the 6c site is probably due to the smallest overlap

TABLE II. Refined parameters of rhombohedral and hexagonal phase for $Y_2Fe_{17}N_{3.1}$ at 10 K. Symbols have the same meaning and units as in Table I.

$Y_2Fe_{17}N_{3.1}$		10 K		$R_p=6.21\%$			
Rhombohedral			$R_I=2.97\%$	$R_F=1.97\%$			
$a=8.6710(3)$ Å			$c=12.7241(4)$ Å				
Atom	Site	n	x	y	z	B	m
Y	6c	1.0	0	0	0.338(1)	0.85(4)	
Fe(1)	6c	1.0	0	0	0.0949(6)	0.202(7)	2.86(5)
Fe(2)	9d	1.0	0.5	0	0.5	0.202	2.12(8)
Fe(3)	18f	1.0	0.2829(5)	0	0	0.202	2.01(4)
Fe(4)	18h	1.0	0.1703(3)	−0.1703	0.4860(4)	0.202	2.41(5)
N(1)	9e	0.995(5)	0.5	0	0	0.65(5)	
N(2)	18g	0.039(2)	0.08(1)	0	0.5	0.65	
Hexagonal			$R_I=3.65\%$	$R_F=2.42\%$			
$a=8.644(2)$ Å			$c=8.495(5)$ Å				
Atom	Site	n	x	y	z	B	m
Y	2b	1.0	0	0	0.25	0.85	
Y	2d	1.0	0.3333	0.6667	0.75	0.85	
Fe(1)	4f	1.0	0.3333	0.6667	0.13(1)	0.202	2.86
Fe(2)	6g	1.0	0.5	0	0	0.202	2.12
Fe(3)	12j	1.0	0.308(9)	0.92(1)	0.25	0.202	2.01
Fe(4)	12k	1.0	0.166(6)	0.333	0.983(7)	0.202	2.41
N(1)	6h	0.995	0.844(8)	1.69	0.25	0.65	
N(2)	12i	0.039	0.1465	0	0	0.65	

of 3d-electron wave functions of iron atoms, because the average Fe-Fe distance between Fe atoms at the 6c site and the other near-neighboring sites is the largest relative to the others. On the contrary, the small values of the Fe moments in the 9d and 18h sites ($1.88\mu_B$ and $1.87\mu_B$) in Y_2Fe_{17} are probably due to a relatively large overlap of 3d-electron wave functions owing to shorter near-neighboring Fe-Fe distances on average. Here it is to be noted that the magnitude of the Fe moments does not correlate with the nearest-neighboring Fe-Y distances. This may be due to the fact that the Fe-Y distance is much longer than the Fe-Fe distance on average. When the N atoms occupy the 9e interstitial site, all Fe moments probably increase due to a reduction in the Fe-Fe overlap caused by the increase in the average Fe-Fe distance on all sites. Furthermore, the magnetic moment of the 18f-Fe atoms which are the nearest to the 9e-N atoms is the lowest ($2.01\mu_B$) owing to the hybridizations between the Fe-3d states and N 2p states. On the contrary, the 6c-Fe atoms which are the farthest from the 9e-N atoms have the highest magnetic moment ($2.86\mu_B$).

Calculated moments of iron atoms located in the different sites and the total magnetic moment per formula unit in the rhombohedral form of Y_2Fe_{17} and $Y_2Fe_{17}N_3$ by Coehoorn,[29] Ching *et al.*,[31] and Asano and Yamaguchi[32] are given in

TABLE III. Magnetic moments on different atomic sites and the total moment per formula unit m_T in Y_2Fe_{17} and $Y_2Fe_{17}N_{3.1}$ at 10 K. The calculated data are taken from Refs. 29, 31, and 32.

Compound	m_Y (μ_B)	m_{Fe} (μ_B)				m_N (μ_B)		
Rhombohedral	6c	6c	9d	18f	18h	9e	m_T (μ_B/f.u.)	Method
Y_2Fe_{17} (expt)	0	2.23(5)	1.88(6)	1.94(2)	1.87(4)		33.0(2)	neutron, 10 K
Y_2Fe_{17} (expt)							33.6	magnetization, 4.2 K
Y_2Fe_{17} (calc)	−0.29	2.29	1.91	2.25	1.97		35.1	scASW,[a] 0 K
Y_2Fe_{17} (calc)	−0.63	2.52	2.05	2.37	2.10		36.8	scOLCAO,[b] 0 K
Y_2Fe_{17} (calc)	−0.34	2.53	1.51	2.10	1.98		33.4	LMTO-ASA,[c] 0 K
$Y_2Fe_{17}N_{3.1}$ (expt)	0	2.86(5)	2.12(8)	2.01(4)	2.41(5)	0	38.6(3)	neutron, 10 K
$Y_2Fe_{17}N_{3.1}$ (expt)							38.7	magnetization, 4.2 K
$Y_2Fe_{17}N_3$ (calc)	−0.46	2.55	2.50	2.02	2.31	−0.07	37.5	scOLCAO,[b] 0 K
$Y_2Fe_{17}N_3$ (calc)	−0.29	2.66	2.42	1.94	2.30	0.05	37.6	LMTO-ASA,[c] 0 K

[a]Reference 29.
[b]Reference 31.
[c]Reference 32.

TABLE IV. Interatomic distance (Å) of rhombohedral Y_2Fe_{17} and $Y_2Fe_{17}N_{3.1}$ at 10 K. Symbol M is the multiplicity of each distance.

Bond	M	Y_2Fe_{17}	$Y_2Fe_{17}N_{3.1}$
Y-Fe(3)f	×6	3.009(1)	3.132(2)
Y-Fe(1)c	×1	3.054(8)	3.09(2)
Y-Fe(4)h	×3	3.086(5)	3.16(1)
Y-Fe(4)h	×3	3.201(5)	3.180(8)
Y-Fe(4)h	×3	3.222(5)	3.40(1)
Y-Fe(2)d	×3	3.278(5)	3.315(8)
Y-N(1)e	×3		2.5037(3)
Fe(1)c-Fe(1)c	×1	2.38(1)	2.41(2)
Fe(1)c-Fe(2)d	×3	2.607(2)	2.665(3)
Fe(1)c-Fe(4)h	×3	2.639(4)	2.681(6)
Fe(1)c-Fe(3)f	×6	2.780(3)	2.734(5)
Fe(1)c-Y	×1	3.054(8)	3.09(1)
Fe(1)c-N(1)e	×3		3.933(6)
Fe(2)d-Fe(3)f	×4	2.4384(4)	2.4790(5)
Fe(2)d-Fe(4)h	×4	2.452(2)	2.483(2)
Fe(2)d-Fe(1)c	×2	2.607(2)	2.665(3)
Fe(2)d-Y	×2	3.278(5)	3.315(8)
Fe(2)d-N(1)e	×4		3.2807(1)
Fe(3)f-Fe(2)d	×2	2.4384(4)	2.4790(5)
Fe(3)f-Fe(3)f	×2	2.511(2)	2.453(4)
Fe(3)f-Fe(4)h	×2	2.531(3)	2.626(4)
Fe(3)f-Fe(4)h	×2	2.622(3)	2.705(5)
Fe(3)f-Fe(1)c	×2	2.780(3)	2.734(5)
Fe(3)f-Y	×2	3.009(1)	3.132(3)
Fe(3)f-Fe(3)f	×1	3.476(5)	3.764(8)
Fe(3)f-N(1)e	×1		1.882(4)
Fe(4)h-Fe(2)d	×2	2.452(2)	2.483(2)
Fe(4)h-Fe(4)h	×2	2.471(3)	2.583(5)
Fe(3)h-Fe(3)f	×2	2.531(3)	2.626(4)
Fe(3)h-Fe(3)f	×2	2.622(3)	2.705(4)
Fe(4)h-Fe(1)c	×1	2.639(4)	2.681(6)
Fe(4)h-Y	×1	3.086(5)	3.16(1)
Fe(4)h-Y	×1	3.201(5)	3.180(8)
Fe(4)h-Y	×1	3.222(5)	3.40(1)
Fe(4)h-N(1)e	×1		1.943(4)
N(1)e-Fe(3)f	×2		1.882(4)
N(1)e-Fe(4)h	×2		1.943(4)
N(1)e-Y	×2		2.5037(3)

Table III (unfortunately, no ^{57}Fe Mössbauer data for rhombohedral Y_2Fe_{17} and $Y_2Fe_{17}N_3$ are available for discussion). There is a substantial correspondence between the experimental and the calculated values at the same Fe sites. However, the results obtained by the calculation are in a little disagreement with our experimental data in detail. Experimentally, a strong enhancement of the 6c-Fe moment and a slight increase in the 18f-Fe moment are recognized upon nitrogenation. On the contrary, the calculations shows that the 6c-Fe moment being the farthest from N atoms slightly increases upon nitrogen uptake, but the moment of 18f-Fe atoms with the N nearest neighbors in the nitride decreases due to the strong hybridizations between the Fe 3d state and N 2p state. We believe that it is necessary to sophisticate the electronic band-structure calculation for understanding the change as microscopic magnetism upon nitrogenation.

TABLE V. Average Fe-Fe interatomic distance (Å) of rhombohedral Y_2Fe_{17} and $Y_2Fe_{17}N_{3.1}$ at 10 K.

Site	Y_2Fe_{17}	$Y_2Fe_{17}N_{3.1}$
Fe(1)c	2.68	2.68
Fe(2)d	2.478	2.518(1)
Fe(3)f	2.658(1)	2.705(2)
Fe(4)h	2.532(1)	2.608(2)

VI. CONCLUSION

In this work, we carefully prepared a almost single-phased rhombohedral Y_2Fe_{17} by annealing at 1393 K for 2 weeks. The $Y_2Fe_{17}N_{3.1}$ nitride was synthesized by a high-pressure nitrogenation method. Using these samples, we performed high-resolution neutron powder diffraction studies at 10 K and analyzed the diffraction data by means of the Rietveld method. It indicates that the N atoms fully occupy the 9e interstitial site (99.5%) and a small amount of N atoms also locates in the 18g interstitial site (3.9%) in the nitride $Y_2Fe_{17}N_{3.1}$. The chemical formula of the nitride estimated from the occupation factors was $Y_2Fe_{17}N_{3.2(1)}$, which is nearly equal to that determined from mass increase. Upon nitrogenation, the lattice parameters a and c at 10 K increase by 2.0% and 2.4%, respectively, without changing the crystallographic symmetry of the host compound. The Fe moments at the 9d and 18h sites are estimated to be $1.88\mu_B$ and $1.87\mu_B$, respectively, which are smaller than the averaged Fe moment, indicating a large overlap of the wave function of the Fe 3d electron due to shorter neighboring Fe-Fe distances in Y_2Fe_{17} on average. On the other hand, the 6c-Fe atoms which are the farthest Fe-Fe atoms on average have the highest magnetic moment ($2.23\mu_B$) due to the smallest overlap of the wave function of the Fe 3d electron. The introduction of N atoms into the host compound leads to the strong modification of the Fe magnetic moments as well as the concomitant lattice expansion. The magnetic moment of the 18f-Fe atoms which are the nearest to the 9e-N atoms in nitride has the lowest value ($2.01\mu_B$), while the magnetic moment of the 6c-Fe atoms which are the farthest from the 9e-N atoms has the highest value ($2.86\mu_B$). The results obtained by our neutron diffraction experiment are substantially in agreement with the results of electronic band-structure calculations.

ACKNOWLEDGMENTS

The authors are grateful to Y. Shimojyo for his technical assistance in the neutron diffraction experiments and the people working at the Department of Research Reactor of Japan Atomic Energy Research Institute for their supports at JRR-3M. We also thank Dr. Y. Ono for his technical assistance in setting to RIETAN program.

[1] A. Iandelli and A. Palenzona, in *Handbook on the Physics and Chemistry of Rare Earths*, edited by K. A. Gschneidner, Jr. and L. Eyring (North-Holland, Amsterdam, 1979), Vol. 2, Chap. 13, p. 1.
[2] S. S. Jaswal, W. B. Yelon, G. C. Hadjipanayis, Y. Z. Wang, and D. J. Sellmyer, Phys. Rev. Lett. **67**, 644 (1991).
[3] J. M. D. Coey and H. Sun, J. Magn. Magn. Mater. **87**, L251 (1990).
[4] M. Katter, J. Wecker, C. Kuhrt, L. Schultz, and R. Grössinger, J. Magn. Magn. Mater. **117**, 419 (1992).
[5] H. Fujii and H. Sun, in *Handbook of Magnetic Materials*, edited by K. H. J. Buschow (North-Holland, Amsterdam, 1995), Vol. 9, Chap. 3, p. 303.
[6] B. P. Hu, H. S. Li, H. Sun, and J. M. D. Coey, J. Phys. Condens. Matter **3**, 3983 (1991).
[7] Q. N. Qi, H. Sun, R. Skomski, and J. M. D. Coey, Phys. Rev. B **45**, 12 278 (1992).
[8] O. Isnard, S. Miraglia, J. L. Soubeyroux, and D. Fruchart, J. Alloys Compounds **190**, 129 (1992).
[9] R. M. Ibberson, O. Moze, T. H. Jacobs, and K. H. J. Buschow, J. Phys. Condens. Matter **3**, 1219 (1991).
[10] S. Miraglia, J. L. Soubeyroux, C. Kolbeck, O. Isnard, D. Fruchart, and M. Guillot, J. Less-Common Met. **171**, 51 (1991).
[11] Y. C. Yang, X. D. Zhang, L. S. Kong, Q. Pan, J. L. Yang, Y. F. Ding, B. S. Zhang, C. T. Ye, and L. Jin, J. Appl. Phys. **70**, 6018 (1991).
[12] W. B. Yelon and G. C. Hadjipanayis, IEEE Trans. Magn. **MAG-28**, 2316 (1992).
[13] T. Kajitani, Y. Morii, S. Funahashi, T. Iriyama, K. Kobayashi, H. Kato, Y. Nakagawa, and K. Hiraya, J. Appl. Phys. **73**, 6032 (1993).
[14] O. Isnard, J. L. Soubeyroux, S. Miraglia, D. Fruchart, L. M. Garcia, and J. Bartolomé, Physica B **180–181**, 624 (1992).
[15] Q. W. Yan, P. L. Zhang, Y. N. Wei, K. Sun, B. P. Hu, Y. Z. Wang, G. C. Liu, C. Gau, and Y. F. Cheng, Phys. Rev. B **48**, 2878 (1993).
[16] O. Isnard, S. Miraglia, J. L. Soubeyroux, D. Fruchart, and J. Pannetier, Phys. Rev. B **45**, 2920 (1992).
[17] O. Isnard, S. Miraglia, J. L. Soubeyroux, D. Fruchart, J. Deportes, and K. H. J. Buschow, J. Phys. Condens. Matter **5**, 5481 (1993).
[18] T. Kajitani, Y. Morii, T. Iriyama, and H. Kato, Physica B **213–214**, 294 (1995).
[19] Y. P. Li, H. S. Li, and J. M. D. Coey, Phys. Status Solidi. B **166**, K107 (1991).
[20] T. Beuerle and M. Fahnle, Phys. Status Solidi B **147**, 257 (1992).
[21] D. Givord, R. Lemaire, J. M. Moreau, and E. Roudaut, J. Less-Common Met. **29**, 361 (1972).
[22] A. N. Christensen and R. G. Hazell, Acta Chem. Scand. A **34**, 455 (1980).
[23] H. Fujii, M. Akayama, K. Nakao, and K. Tatami, J. Alloys Compounds **219**, 10 (1995).
[24] H. Fujii, K. Tatami, and K. Koyama, J. Alloys Compounds **236**, 156 (1996).
[25] Y. Morii, K. Fuchizaki, S. Funahashi, N. Minakawa, Y. Shimojyo, and A. Ishida, in *Proceedings of the 4th International Symposium on Advanced Nuclear Energy Research*, 1992, Mito, Japan, edited by T. Kondo (Japan Atomic Energy Research Institute, Ibaraki, 1992), p. 280.
[26] F. Izumi, in *The Rietveld Method*, edited by R. A. Young (Oxford University Press, Oxford, 1993), Chap. 13.
[27] Y. I. Kim and F. Izumi, J. Ceram. Soc. Jpn. **102**, 401 (1994).
[28] P. J. Brown, in *The International Tables for Crystallography*, edited by A. J. C. Wilson (Kluwer, Dordrecht, 1995), Vol. C, Chap. 4, p. 391.
[29] R. Coehoorn, Phys. Rev. B **39**, 13 072 (1989).
[30] T. Beuerle, P. Braun, and M. Fähnle, J. Magn. Magn. Mater. **94**, L11 (1991).
[31] W. Y. Ching, M. Z. Huang, and X. F. Zhong, J. Appl. Phys. **76**, 6047 (1994).
[32] S. Asano and M. Yamaguchi, Physica B (to be published).